Effect of Sn O 2 addition on the dielectric properties of Ba 2 Ti 9 O 20 ceramics in the high-frequency regime

Hsiang-Lin Liu, Hsin-I Chen, Yuan-Tai Tzeng, Chia-Ta Chia, Kuo-Chien Hsu, Chen-Chung Chi, Chi-Ben Chang, Keh-Chyang Leou, and I-Nan Lin

---

Articles you may be interested in

First-principles study of the dielectric properties of Ba (Zn 1 / 3 Nb 2 / 3) O 3 and Ba (Mg 1 / 3 Nb 2 / 3) O 3
J. Appl. Phys. **105**, 034111 (2009); 10.1063/1.3077191

Intrinsic dielectric and spectroscopic behavior of perovskite Ba (Ni 1∕3 Nb 2∕3) O 3 – Ba (Zn 1∕3 Nb 2∕3) O 3 microwave dielectric ceramics
J. Appl. Phys. **102**, 044112 (2007); 10.1063/1.2770870

Infrared reflection spectra of Ba 6 − 3 x Sm 8 + 2 x Ti 18 O 54 (x = 0.5 , 0.67, and 0.75) microwave dielectric ceramics
J. Appl. Phys. **101**, 064103 (2007); 10.1063/1.2710299

Raman spectra of Nd∕Sn cosubstituted Ba 6 − 3 x Sm 8 + 2 x Ti 18 O 54 microwave dielectric ceramics
J. Appl. Phys. **96**, 5683 (2004); 10.1063/1.1805186

High frequency dielectric properties of A 5 B 4 O 15 microwave ceramics
J. Appl. Phys. **89**, 3900 (2001); 10.1063/1.1351873

Effect of SnO₂ addition on the dielectric properties of Ba₂Ti₉O₂₀ ceramics in the high-frequency regime

Hsiang-Lin Liu,[a)] Hsin-I Chen, Yuan-Tai Tzeng, and Chia-Ta Chia
Department of Physics, National Taiwan Normal University, Taipei 116, Taiwan

Kuo-Chien Hsu and Chen-Chung Chi
Department of Physics, National Tsing Hua University, Hsinchu 300, Taiwan

Chi-Ben Chang and Keh-Chyang Leou
Department of Engineering and System Science, National Tsing Hua University, Hsinchu 300, Taiwan

I-Nan Lin
Department of Physics, Tamkang University, Tamsui 251, Taiwan

The effect of SnO₂ addition on the high-frequency dielectric properties of Ba₂Ti₉O₂₀ ceramics has been investigated using terahertz time-domain spectroscopy, far-infrared (FIR) reflectivity, and Raman-scattering measurements. The dielectric constants determined from the terahertz and FIR spectra are smaller than that taken in the microwave frequency region. In contrast, the increase of the dielectric loss with increasing frequency is due to some resonance modes above 1 THz. Importantly, our data clearly show that the SnO₂ (2.4 mole %) addition degraded the dielectric properties of Ba₂Ti₉O₂₀ ceramics, which is ascribed to the deterioration on the coherency of lattice vibrational characteristics for these materials. © *2006 American Institute of Physics.*
[DOI: 10.1063/1.2363605]

I. INTRODUCTION

Generally, the dielectric losses in the microwave dielectrics could be induced either intrinsically or extrinsically. The intrinsic losses are related to the material compositions and crystal structures, which are less process dependent, whereas the extrinsic losses are associated with the defects (vacancies and impurities), structural disorders, porosities, or second phases, which vary with the processing parameters markedly. The investigations on the dielectric properties of these materials are sometimes controversial, which is primarily due to the interference of the extrinsic dielectric loss on the measured dielectric characteristics. A better understanding of these phenomena requires carefully exploring their high-frequency dielectric properties, since the intrinsic losses are overwhelmingly stronger than the extrinsic ones in the far-infrared regime.[1–4] Indeed, a number of recent experiments in the submillimeter and far-infrared frequency ranges have provided such evidence.[5–10]

A Ba₂Ti₉O₂₀ phase was reported by Jonker and Kwestroo in a BaO–TiO₂–SnO₂ ternary system.[11] It possesses marvelous microwave dielectric properties, including the high dielectric constant and large quality factor.[12] Since then the modification on the microwave properties of Ba₂Ti₉O₂₀ with the addition of dopants was widely investigated.[13–17] However, the reproducible results have not been found, which is mainly due to the difficulty in forming single phase hollanditelike structured Ba₂Ti₉O₂₀ materials. Secondary phases, such as BaTi₄O₉ or BaTi₅O₁₁, are formed preferentially in the calcinations of a BaO–TiO₂ mixture[18] and hindered the formation of a hollanditelike structured Ba₂Ti₉O₂₀

phase. In order to circumvent this kind of difficulty, the nanosized BaTiO₃ powders were used to mix with proper amount of TiO₂ and then processed by a conventional mixed oxide procedure. The Ba₂Ti₉O₂₀ powders possessing both high precision in composition and high sinterability can be obtained. Consequently, the microwave dielectric properties of the sintered Ba₂Ti₉O₂₀ materials can be improved. Furthermore, the SnO₂ addition was observed to facilitate the formation of a hollanditelike phase, improving the microwave dielectric properties for the Ba₂Ti₉O₂₀ materials.[11] The question that remained is how these additives modify the fundamental characteristics of the materials. There is an urgent need to throw more light on whether they improve the microwave dielectric properties of the Ba₂Ti₉O₂₀ materials intrinsically or alter these properties via enhancing the phase transformation behavior.

In this paper, we present the terahertz time-domain spectroscopy, far-infrared reflectivity, and Raman-scattering measurements of Ba₂Ti₉O₂₀ ceramics in an effort to study the effect of SnO₂ addition on the high-frequency dielectric properties of these materials. It is found that the incorporation of SnO₂ additives leads to a suppression of the high-frequency dielectric constant but increases the dielectric loss in comparison to the undoped samples. This behavior is opposite to the trend in the microwave regime. In addition, several infrared- and Raman-active phonon peaks show a broadening in their linewidths for the SnO₂-doped samples, reflecting that the coherency in these vibrational modes is degraded. Our data support the point of view that the SnO₂ additives modify the microwave dielectric properties of Ba₂Ti₉O₂₀ ceramics extrinsically, rather than intrinsically.

---

a)Electronic mail: hliu@phy.ntnu.edu.tw

100, 094104-1

II. EXPERIMENT

Nanosized $BaTiO_3$ powders (≈ 50 nm) were mixed with nanosized TiO_2 powders (≈ 100 nm) in a nominal composition of $Ba_2Ti_9O_{20}$. The mixtures were calcined at 950 °C for 4 h in air, followed by a pulverization-granulation-pelletization process, and then were sintered at 1350 °C for 4 h in air. The morphology of the as-prepared $Ba_2Ti_9O_{20}$ powders and the microstructure of the sintered $Ba_2Ti_9O_{20}$ samples were examined using scanning electron microscopy (SEM) (JEOL 6700F). The crystal structures of the calcined powders and sintered samples were checked by the x-ray powder diffraction (Rigaku D/max-II). The density of the sintered samples was determined from the Archimedes method. The microwave dielectric constant and the quality factor of the $Ba_2Ti_9O_{20}$ samples were measured using a cavity method at 6 GHz.

The terahertz time-domain spectroscopy is used to determine the complex transmission function of the samples.[9,10] The terahertz transient produced by illuminating the GaAs-photoconducting antenna with ultrashort laser pulses was directed onto the samples, serving as pump pulse. The scattered terahertz transient was collected and reflected by an off-axis paraboloidal mirror and then was focused onto the electro-optic crystal. In this terahertz experiment, reference data were first obtained without the sample between the transmitter and the receiver. Subsequently, a sample was introduced in the path of the terahertz beam and a second set of data was obtained. The spectra of terahertz transient can be obtained by applying a fast Fourier transform to the time-domain wave form. Dividing the spectra obtained with a sample by the spectra obtained without a sample yields the transmission function $t(\omega)$ of the sample

$$t(\omega) = \left[\frac{4N_s}{(N_s + 1)^2} \right] \exp[i(k_s - k_v)d], \qquad (1)$$

where $N_s = n + ik$ is the complex refraction index of the sample, $k_s = \omega N_s/c$, $k_v = \omega/c$, ω is the frequency, d is the thickness of the sample, and c is the speed of light in vacuum. Equation (1) can be solved numerically.

The samples were polished with 0.05 μm grain size Al_2O_3 powders until an optically reflecting surface was achieved. Near-normal infrared reflectance measurements were then carried out at room temperature. A Bruker IFS 66v Fourier transform infrared spectrometer was used in the far-infrared and midinfrared regions ($40–6000$ cm^{-1}). The modulated light beam from the spectrometer was focused onto either the sample or a Au reference mirror, and the reflected beam was directed onto a detector appropriate for the frequency range studied. The different sources and detectors used in these studies provided substantial spectral overlap, and the reflectance mismatch between adjacent spectral ranges was less than 1%. Spectral resolution is 2 cm^{-1}. The optical properties [i.e., the complex conductivity $\sigma(\omega) = \sigma_1(\omega) + i\sigma_2(\omega)$ or dielectric constant $\epsilon(\omega) = 1 + 4\pi i \sigma(\omega)/\omega$] were calculated from a Kramers-Kronig analysis of the reflectance data.[19] To perform these transformations one needs to extrapolate the reflectance at both low and high frequencies. At low frequencies the extension was done by modeling the reflectance using the Lorentz model and using the fitted results to extend the reflectance below the lowest frequency measured in the experiment. The high-frequency extrapolations were done by using a weak power law dependence $R \approx \omega^{-s}$ with $s \approx 1–2$.

The room-temperature Raman spectra were measured with 514.5 nm photons from an Ar^+ ion laser. The linearly polarized light was focused on the sample through a $100\times$ optical microscope objective [0.95 numerical aperture (NA)] with a spatial resolution of <1 μm in a backscattering geometry. The laser power used was less than 1.5 mW. The scattered light without polarization analysis was collected and dispersed by a Dilor XY 800 triple spectrometer equipped with 1800 grooves/mm gratings and a liquid-nitrogen cooled 1024 pixel wide charge-coupled detector. The spectral resolution of these instruments was typically less than 1 cm^{-1}. All Raman spectra were corrected for the frequency-dependent response of the system and for the optical response of the materials.

III. RESULTS AND DISCUSSION

A conventional mixed oxide route for synthesizing hollanditelike structured $Ba_2Ti_9O_{20}$ via calcinations of $BaCO_3$ and TiO_2 mixtures is practically not possible to circumvent the occurrence of residual secondary phases, even when doped with 2.4 mole % SnO_2. It requires high processing temperature (1350 °C for 4 h) to completely eliminate the presence of residual phase and reach high density materials. Thus obtained materials possess relatively low dielectric constant $K \approx 36$ and unsatisfactory quality factor $Q \times f \approx 28$ THz.

In contrast, when the nanosized perovskite $BaTiO_3$ powders (≈ 50 nm) were utilized as starting materials, the phase transformation kinetics was pronouncedly enhanced. Figure 1(a) shows the diffraction profile for the $x = 0.00$ compound at room temperature. All the reflections can be indexed and no impurity phases are apparent above the background level. It is found that the powders were crystallized to form a $BaTi_4O_9$ phase when calcined at 1000 °C for 6 h. These powders were completely converted into a hollanditelike structure when calcined at 1100 °C for 6 h. However, both these two kinds of powders can be effectively densified by sintering the pressed pellets at 1350 °C for 4 h, possessing a hollanditelike structure, regardless of the phase constituents of the presinter powders.

The nano-$BaTiO_3$ derived materials show markedly superior microwave dielectric properties to the conventionally processed ones prepared from the $BaCO_3 + TiO_2$ mixture, possessing the same high density. They are $K \approx 38.5$ and $Q \times f \approx 31.5$ THz for the nano-$BaTiO_3$-derived materials and $K \approx 36$ and $Q \times f \approx 28$ THz for the $BaCO_3$-derived ones. The beneficial effect of using nanosized $BaTiO_3$ powders on facilitating the reaction process and on improving the microwave dielectric properties of $Ba_2Ti_9O_{20}$ materials is clearly demonstrated. Presumably, the inferior microwave dielectric properties for the $BaCO_3$-derived materials have a strong
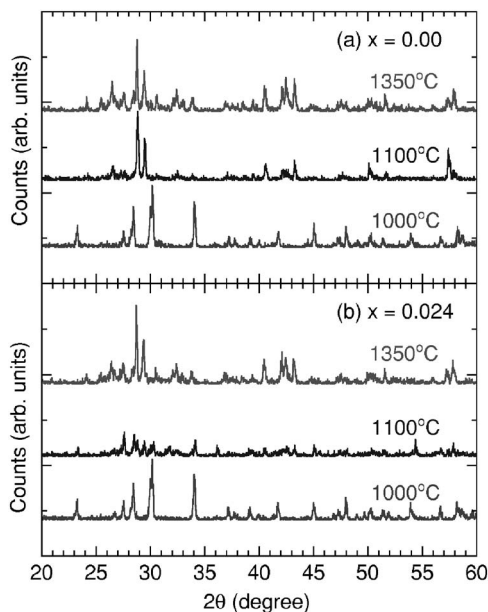
FIG. 1. The x-ray diffraction patterns of the as-calcined (1000 °C for 6 h or 1100 °C for 6 h) powders and sintered (1350 °C for 4 h) ceramics, which were prepared from the nanosized $BaTiO_3 + TiO_2$ mixture, containing (a) no SnO_2 additives and (b) 2.4 mole % SnO_2 additives.
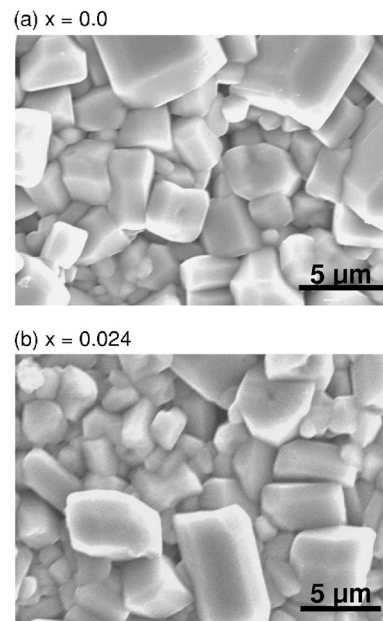

FIG. 2. Typical SEM micrograph of the $Ba_2Ti_9O_{20}$ materials sintered at 1350 °C for 4 h, which contain (a) no SnO_2 additives and (b) 2.4 mole % SnO_2 additives.

correlation with the nonuniform microstructure for the materials due to the complicated phase transformations that occurred in sintering periods.

Addition of 2.4 mole % SnO_2 into the materials does not markedly modify the phase transformation kinetics for the nano-$BaTiO_3$ derived materials. It is interesting to note that calcining the powders at 1100 °C for 6 h is still not able to eliminate the presence of $BaTi_4O_9$ phase residue preferentially formed, as shown in Fig. 1(b). It needs 1150 °C for 6 h to completely convert the nano-$BaTiO_3 + TiO_2$ mixture into hollanditelike phase (not shown). Again, the sintered materials are all hollanditelike, whether the as-calcined powders contain the secondary phase or not. Figure 2 shows typical SEM images of $Ba_2Ti_9O_{20}$ materials sintered at 1350 °C for 4 h without and with 2.4 mole % SnO_2 additives. The granular structures of these two samples are very alike. The grains are short rod shaped with small aspect ratio (3×6 μm^2).

Figure 3 displays the real and imaginary parts of the dielectric constant obtained by terahertz time-domain spectroscopy for the $x=0.00$ and 0.024 samples. One first observes that the real part of the dielectric constant $\epsilon_1(\omega)$ of these materials hardly changes in the 0.1–0.6 THz regime. It is ≈ 32.5 for the undoped and ≈ 31.5 for the SnO_2-doped $Ba_2Ti_9O_{20}$ materials. These values are smaller than those measured in the microwave frequency regime (see Table I). Second, there appears several resonance peaks in the imaginary part of the dielectric constant $\epsilon_2(\omega)$ for the undoped sample. The presence of these resonance features in the undoped sample would contribute additional dielectric polarization, as predicted by the Kramers-Kronig theory. Notably, the addition of SnO_2 into $Ba_2Ti_9O_{20}$ materials markedly broadens these resonance peaks, implying that the coherence of collective motion of the lattices is deteriorated. Third, the calculated quality factor $Q=\epsilon_1/\epsilon_2$ at 0.5 THz is ≈ 52.8 for the undoped and ≈ 40 for the SnO_2-doped $Ba_2Ti_9O_{20}$ mate-

rials, which correspond to $Q \times f \approx 26.4$ and ≈ 20 THz, respectively. It is important to note that the quality factor measured at terahertz frequency is markedly smaller than those measured at microwave frequency. The addition of 2.4 mole % SnO_2 pronouncedly modifies the terahertz dielectric properties of these materials.

The measured infrared reflectance spectra are shown in Fig. 4. In all cases, the spectra of the samples reveal the characteristic of an insulator at low frequencies. A number of phonon features are observed in the far-infrared region, which needs the first-principles calculation to unambigu-
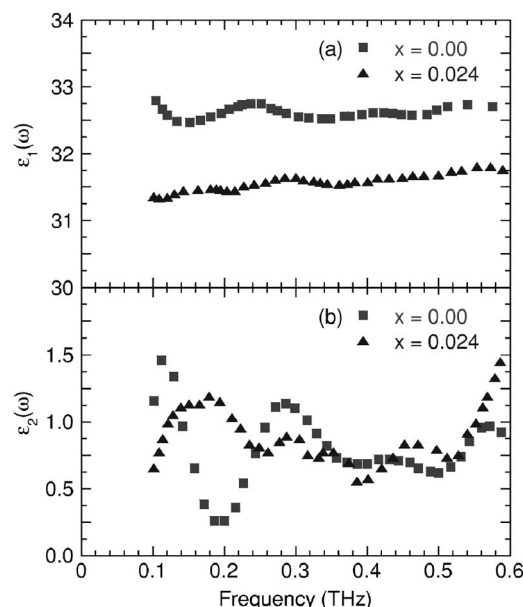

FIG. 3. The frequency dependence of (a) the real part and (b) the imaginary part of the dielectric constant of $Ba_2Ti_9O_{20}$ materials sintered at 1350 °C for 4 h, containing no SnO_2 additives and 2.4 mole % SnO_2 additives in 0.1–0.6 THz.

TABLE I. The dielectric properties of the $x=0.00$ and 0.024 compounds (Ref. 21).

	K	$Q \times f$ (THz)
$x=0.00$		
$\omega=6.0$ GHz (microwave)	38.5	31.5
$\omega=0.5$ THz (terahertz)	32.8	26.4
$\omega=1.0$ THz (far infrared)	32.0	13.0
$x=0.024$		
$\omega=6.0$ GHz (microwave)	39.0	31.0
$\omega=0.5$ THz (terahertz)	31.4	20.0
$\omega=1.0$ THz (far infrared)	31.0	7.0

TABLE II. Parameters of a Lorentzian fit for the optical reflectance data.

	$x=0.00$			$x=0.024$	
ω_{pj} (cm^{-1})	ω_j (cm^{-1})	γ_j (cm^{-1})	ω_{pj} (cm^{-1})	ω_j (cm^{-1})	γ_j (cm^{-1})
86	71	16	100	72	20
163	97	19	180	97	25
59	128	11	60	128	15
103	160	16	103	160	20
549	230	61	586	230	80
150	256	10	120	256	15
743	286	40	620	286	48
132	335	13	120	337	20
857	396	89	770	396	100
270	465	37	220	467	40
118	492	15	70	493	20
775	551	105	720	558	122
200	622	25	180	624	32
400	785	122	427	785	163
$\epsilon_\infty=$	5.8	$\cdots$	$\cdots$	5.2	$\cdots$

ously identify each resonance modes. The linewidth and intensity of these phonon peaks are perturbed to some extent by the addition of 2.4 mole % SnO$_2$, reflecting the degraded coherence of the lattice vibrational characteristics of the Ba$_2$Ti$_9$O$_{20}$ materials. In order to examine this behavior more quantitatively, we fit these phonon modes using a standard Lorentzian profile,[19,20]

$$\epsilon(\omega) = \sum_{j=1}^{N} \frac{\omega_{pj}^2}{\omega_j^2 - \omega^2 - i\omega\gamma_j} + \epsilon_\infty, \qquad (2)$$

where ω_j, γ_j, and ω_{pj} are the frequency, damping, and oscillator strength of the jth Lorentzian contribution, respectively, and ϵ_∞ is the high-frequency limit of $\epsilon(\omega)$ which includes interband transitions at frequencies above the measured range. The parameters used to fit the measured optical data are listed in Table II. The spectrum is well reproduced by considering 14 Lorentzian oscillators representing the phononic excitations. ϵ_∞ is ≈ 5.8 for $x=0.00$ and ϵ_∞ is ≈ 5.2 for $x=0.024$. We notice that all the modes of the SnO$_2$-doped sample exhibit a broadening of their linewidths in comparison to the undoped sample, illustrating that addition of 2.4 mole % SnO$_2$ into Ba$_2$Ti$_9$O$_{20}$ materials results in the de-

terioration of the coherence of the lattice degrees of freedom.

The real and imaginary parts of the dielectric constant, calculated by a Kramers-Kronig analysis of the reflectance curves, are presented in Figs. 5(a) and 5(b). The infrared vibrational excitations result in a negative real dielectric function between the transverse (ω_{TO}) and the longitudinal (ω_{LO}) frequencies of each mode. By extrapolating the low-frequency far-infrared data to zero frequency, we estimate the static dielectric constant for $x=0.00$ and 0.024 samples to be $\epsilon_1(0) \approx 32.5$ and 31.4, respectively, which agree very well with the terahertz measurements. In the midinfrared region, a flat $\epsilon_1(\omega)$ can be seen and gives $\epsilon_1=6.0-5.0$. To facilitate the comparison, the insets in Fig. 5 show the real and imaginary
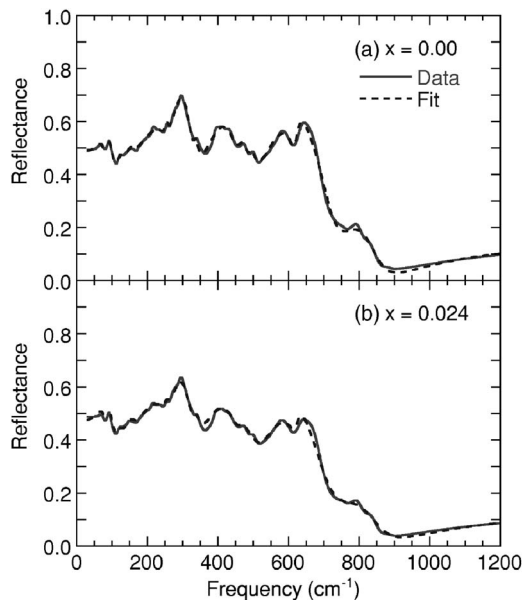

FIG. 4. Room-temperature infrared reflectance spectra (solid lines) of the (a) $x=0.00$ and (b) $x=0.024$ compounds. The dashed lines are the best fits using the Lorentzian model.
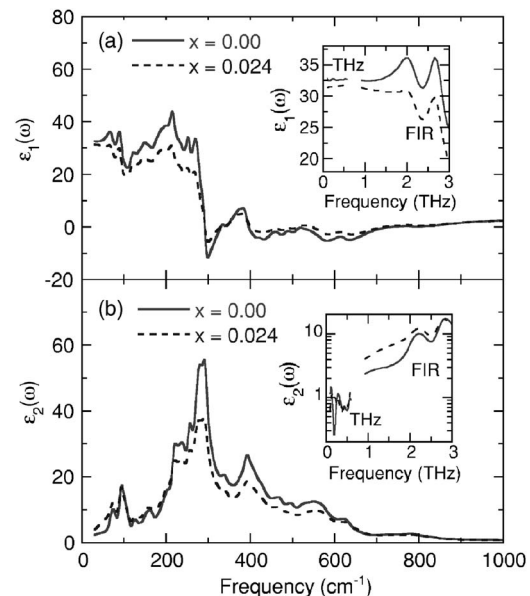

FIG. 5. (a) The real part and (b) the imaginary part of the dielectric constant (from a Kramers-Kronig transformation) for the $x=0.00$ and 0.024 compounds from 30 to 1000 cm^{-1}. Insets show the full spectra of the dielectric constant derived from the terahertz and far-infrared measurements.
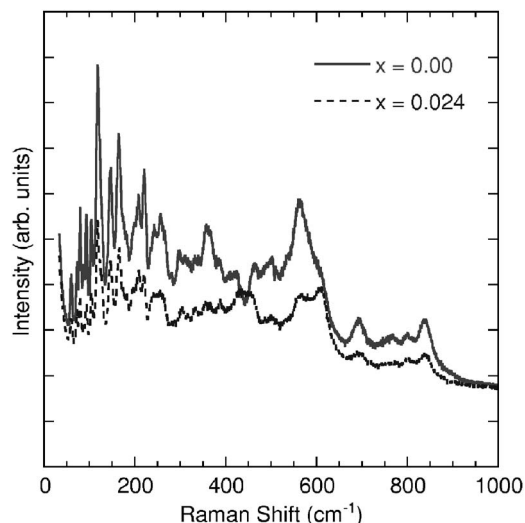
FIG. 6. Raman spectra of $Ba_2Ti_9O_{20}$ materials sintered at 1350 °C for 4 h, containing no SnO_2 additives and 2.4 mole % SnO_2 additives.

parts of the dielectric constant measured in the terahertz and far-infrared frequency regimes. For both samples, the $\epsilon_1(\omega)$ values derived from terahertz are about the same as those measured by far-infrared reflectivity (FIR), implying that the FIR measurements down to 30 cm^{-1} (1.0 THz) are necessary and sufficient to accurately describe the dielectric behavior.

To provide additional information on how the addition of 2.4 mole % SnO_2 modifies the characteristics of the phonon modes so as to understand the dielectric mechanism for $Ba_2Ti_9O_{20}$, we used the Raman-scattering technique to investigate the vibrational properties of these materials. Figure 6 shows the Raman spectra of the $x=0.00$ and 0.024 compounds at room temperature. The spectra of the two samples are composed of optical phonon modes and a broad luminescence background. The phonon response is very complicated due to the high unsymmetry of the hollanditelike crystal structure. To illustrate the detailed changes of the Raman spectra with SnO_2 addition, we fit the phonon peaks in the range of 50–250 cm^{-1} using a standard Lorentzian profile (not shown). It is clear that the phonon peaks for the undoped $Ba_2Ti_9O_{20}$ possess smaller resonance linewidth, which corresponds to a more coherent lattice vibration and a higher quality factor, as compared with those for the SnO_2-doped one. Moreover, addition of SnO_2 results in slight shifting of the resonance frequency toward the larger Raman shifts, indicating the tighter bonding between the cations and the anions and the smaller dielectric constant for the SnO_2-doped materials. These results are consistent with the dielectric properties measured in the terahertz and far-infrared frequency regimes; viz., incorporation of SnO_2 lowers the dielectric constant and degrades the quality factor for the $Ba_2Ti_9O_{20}$ materials.

IV. SUMMARY

The phase transformation kinetics for the formation of a hollanditelike phase is facilitated by using nanosized ($\approx$50 nm) $BaTi_3+TiO_2$ mixtures as starting materials, such that the hollanditelike structured $Ba_2Ti_9O_{20}$ can be obtained

by sintering the materials at 1350 °C for 4 h in air, regardless of the phase constituents in the calcined powders. The effect of SnO_2 addition on the dielectric properties of $Ba_2Ti_9O_{20}$ materials were examined over a wide frequency range from microwave, terahertz, to far infrared. It is found that the high-frequency dielectric constant of the SnO_2-doped materials is lowered, whereas the loss factor is increased. Moreover, the infrared- and Raman-active optical phonons show a slight blueshift accompanying an increase of the linewidths; i.e., the coherence in vibrational modes is degraded due to the SnO_2 additives. Such a trend is contrary to the effect of SnO_2 addition on dielectric properties of $Ba_2Ti_9O_{20}$ in the microwave regime. All of these observables support the suggestion that SnO_2 additives modify the low-frequency dielectric properties extrinsically, rather than intrinsically.

[1]G. O. Rupprecht and R. O. Bell, Phys. Rev. **125**, 1915 (1962).
[2]B. D. Silverman, Phys. Rev. **125**, 1921 (1962).
[3]J. Petzelt *et al.*, Ferroelectrics **93**, 77 (1989).
[4]V. L. Gurevich and A. K. Tagantsev, Adv. Phys. **40**, 719 (1991).
[5]J. Petzelt, R. Zurmuhlen, A. Bell, S. Kamba, G. V. Kozlov, A. A. Volkov, and N. Setter, Ferroelectrics **133**, 205 (1992).
[6]J. Petzelt, S. Kamba, G. V. Kozlov, and A. A. Volkov, Ferroelectrics **176**, 145 (1996).
[7]Y. C. Chen, H. F. Cheng, H. L. Liu, C. T. Chia, and I. N. Lin, J. Appl. Phys. **94**, 3365 (2003).
[8]P. Kuzel and J. Petzelt, Ferroelectrics **239**, 949 (2000).
[9]T. R. Tsai, M. H. Liang, C. T. Hu, C. C. Chi, and I. N. Lin, Jpn. J. Appl. Phys., Part 1 **94**, 5642 (2000).
[10]T. R. Tsai, M. H. Liang, C. T. Hu, C. C. Chi, and I. N. Lin, J. Eur. Ceram. Soc. **21**, 2787 (2001).
[11]G. H. Jonker and W. Kwestroo, J. Am. Ceram. Soc. **41**, 390 (1958).
[12]H. M. O'Bryan, J. Thomson, Jr., and J. K. Plourde, J. Am. Ceram. Soc. **57**, 450 (1974).
[13]H. M. O'Bryan and J. Thomson, Jr., J. Am. Ceram. Soc. **57**, 522 (1974).
[14]G. D. Fallon and B. M. Gatehouse, J. Solid State Chem. **49**, 59 (1983).
[15]H. M. O'Bryan, W. H. Grodkiewicz, and J. L. Bernstein, J. Am. Ceram. Soc. **63**, 309 (1979).
[16]G. Grzinic and L. A. Bursill, J. Solid State Chem. **47**, 151 (1983).
[17]E. Tillmanns, W. Hofmeister, and W. H. Baur, J. Am. Ceram. Soc. **66**, 268 (1983).
[18]J. M. Wu and H. W. Wang, J. Am. Ceram. Soc. **71**, 869 (1988).
[19]F. Wooten, *Optical Properties of Solids* (Academic, New York, 1972).
[20]We notice that a polycrystalline sample is an inhomogeneous medium whose physical properties vary spatially due to crystal-to-crystal orientation. In our samples, a local response can be justified because the grain size (diameter ~0.1 μm after polishing) is much smaller than the wavelength of the light in the range of our interest. Additionally, since $Ba_2Ti_9O_{20}$ has the nearly three-dimensional structure, its optical constants should be nearly isotropic. The Lorentzian fitting analysis could be applied to our polycrystalline samples without much problem.
[21]In our recent separate experiments, we did observe that the microwave dielectric constant (K) and quality factor ($Q\times f$) measured at 6 GHz for the $Ba_2(Ti_{9-x}Sn_x)O_{20}$ materials is modified pronouncedly with the SnO_2 content (x value). With increasing SnO_2 doping, the values of K and $Q\times f$ for $x=0.055$, 0.11, and 0.22 samples are 38.2 and 31 THz, 37 and 30 THz, and 35.5 and 28.5 THz, respectively. It should be noted that all the samples are of very high density [>98% theoretical density (TD)] and of pure hollanditelike phase, possessing a very uniform granular structure.